INTERFACE

rsif.royalsocietypublishing.org

Research

Cite this article: Richardson TO, Gorochowski TE. 2015 Beyond contact-based transmission networks: the role of spatial coincidence. *J. R. Soc. Interface* **12**: 20150705. http://dx.doi.org/10.1098/rsif.2015.0705

Received: 6 August 2015
Accepted: 28 August 2015

Subject Areas:
computational biology, systems biology, biocomplexity

Keywords:
networks, social insects, *Temnothorax albipennis*, communication, epidemic

Authors for correspondence:
Thomas O. Richardson
e-mail: thomas.richardson@unil.ch
Thomas E. Gorochowski
e-mail: teg@mit.edu

†These authors contributed equally to this study.
‡Present address: Department of Biological Engineering, Massachusetts Institute of Technology, Cambridge, MA 02139, USA.

Electronic supplementary material is available at http://dx.doi.org/10.1098/rsif.2015.0705 or via http://rsif.royalsocietypublishing.org.

THE ROYAL SOCIETY PUBLISHING

Beyond contact-based transmission networks: the role of spatial coincidence

Thomas O. Richardson[1,2,3,†] and Thomas E. Gorochowski[4,†,‡]

[1]Department of Ecology and Evolution, University of Lausanne, 1015 Lausanne, Switzerland
[2]Department of Mathematics and Statistics, Bristol Institute of Technology, University of the West of England, Bristol BS16 1QY, UK
[3]School of Biological Sciences, and [4]Bristol Centre for Complexity Sciences, Department of Engineering Mathematics, University of Bristol, Bristol BS8 1UB, UK

TOR, 0000-0002-0220-4897; TEG, 0000-0003-1702-786X

Animal societies rely on interactions between group members to effectively communicate and coordinate their actions. To date, the transmission properties of interaction networks formed by direct physical contacts have been extensively studied for many animal societies and in all cases found to inhibit spreading. Such direct interactions do not, however, represent the only viable pathways. When spreading agents can persist in the environment, indirect transmission via 'same-place, different-time' spatial coincidences becomes possible. Previous studies have neglected these indirect pathways and their role in transmission. Here, we use rock ant colonies, a model social species whose flat nest geometry, coupled with individually tagged workers, allowed us to build temporally and spatially explicit interaction networks in which edges represent either direct physical contacts or indirect spatial coincidences. We show how the addition of indirect pathways allows the network to enhance or inhibit the spreading of different types of agent. This dual-functionality arises from an interplay between the interaction-strength distribution generated by the ants' movement and environmental decay characteristics of the spreading agent. These findings offer a general mechanism for understanding how interaction patterns might be tuned in animal societies to control the simultaneous transmission of harmful and beneficial agents.

1. Introduction

Over the last 20 years, numerous detailed studies of individual behaviour in animal societies have revealed that adaptive collective behaviours, such as flocking, shoaling and swarming, all emerge from numerous localized interactions between group members. Some of the most advanced animal societies are found in the eusocial insects—the ants, bees, wasps and termites—which, although representing only 2% of all insect species, contribute more than 75% of all insect biomass [1]. Life within a social insect colony involves frequent exchanges of information between the workers. These exchanges take place over two major pathways: (i) direct 'same-place, same-time' interactions such as physical contacts [2–7] and (ii) indirect 'same-place, different-time' interactions where workers influence the behaviour of others through modification of the shared environment [8,9]. Depending upon the context, these pathways function to transmit information [2,10], materials [11] or both [12]. A major problem such societies face is that the concentration of so many closely related individuals at a single location renders them particularly vulnerable to disease. It is therefore intuitive to expect that the interaction patterns underlying the social organization should have evolved to facilitate the efficient dissemination of beneficial materials such as food [3] or information-bearing chemicals [10], while also inhibiting the spread of harmful pathogens [13–16] (henceforth we term beneficial materials or information and pathogens as 'agents'). At present, it is far from clear how interaction patterns can be structured in space and time to satisfy these competing requirements, or the mechanisms that animal societies might employ to modulate their propagation.

Most recent work on interaction patterns in humans [17–22], other mammals [23–26] and social insects [3–6,13,14,23,27,28] has focused on building empirical networks derived from sequences of direct interactions. These generally include face-to-face encounters [21] or physical contacts and are often termed 'close proximity interactions' (CPIs) [19]. In all cases, these types of network have been found to inhibit spreading when compared to null-models in which individuals are 'well-mixed' with interactions between individuals being neither biased, preferential nor assortative [4,18–21,29].

Building networks solely from CPIs ignores the fact that when individuals have the potential to deposit agents within the environment, and when those agents show environmental persistence (e.g. pheromones with low evaporation rates in the case of information-carrying materials, or virulent 'sit-and-wait' pathogens [30] in the case of disease), indirect transmission by spatial coincidence becomes possible [31,32]. While researchers of collective animal behaviour have long appreciated that the shared environment can be used as a spatial intermediary for indirect communication [8,9,12, 33–35], biologists are only beginning to quantify the important role of indirect interactions in the transmission of other types of agents, such as pathogens [30,36–40]. The general absence of indirect transmission pathways from previous studies of spreading processes over animal interaction networks (but see [31]), means that the emerging picture of information and disease spread in animal societies is based on an incomplete sampling of the total interaction space.

To address these shortcomings, we developed a modelling framework in which both interaction types are incorporated within a temporally and spatially explicit network abstraction (figure 1*a*). Individuals are represented by vertices and both direct and indirect interactions by directional and weighted edges. Unlike many standard network analyses where repeated interactions on a particular edge are aggregated over time [3,5,6,13,14,22,24,25,27,28,41], we consider the temporal ordering of individual interactions, because the transmission properties of the aggregated network are typically qualitatively different to the underlying temporal network [4,19–21,29].

In our framework, an interaction occurs whenever two ants, *i* and *j*, visit the same location (within a 1 mm threshold; figure 1*a*). Simultaneous visits result in a direct 'same-place, same-time' interaction, whereas a delay between the two visits leads to an indirect 'same-place, different-time' interaction. The time that elapses between the two visits is termed the intersect delay $\tau_{i\to j}$. As the transmission probability for any given interaction will be influenced by the length of this delay, and also the environmental persistence of the agent, we define a time-ordered network in which each interaction defines a single edge whose weight reflects both of these factors (figure 1*a*; Material and methods). To capture the environmental decay that an agent experiences when deposited in the environment, all interactions were assigned weights that decay at a rate α in accordance with the intersect delay $\tau_{i\to j}$ (figure 1; Material and methods). Because there is no delay associated with direct encounters, $\tau_{i\to j} = 0$, transmission via these CPIs is more likely to be successful. Hence, we represented these by maximally weighted edges with a fixed value of 1. All interactions then lie along a continuum with weaker indirect interactions occupying the bulk of the edge-weight distribution and strong direct CPIs representing only a limiting case. It should be noted that indirect spreading via spatial coincidence also constrains the directionality of the edges that represent them. Specifically, as information or material can only propagate forwards in time, indirect interactions are only able to transmit from a sender to receiver, thus edges representing them are uni-directional. By contrast, the simultaneous co-location of individuals during a CPI leads to edges forming in both directions enabling bi-directional transmission. Finally, to quantify how well an agent with a given environmental persistence might propagate over a network, we implemented the commonly used stochastic Susceptible-Infected (SI) epidemic model to simulate agent transmission over the temporal networks [29,42] (Material and methods).

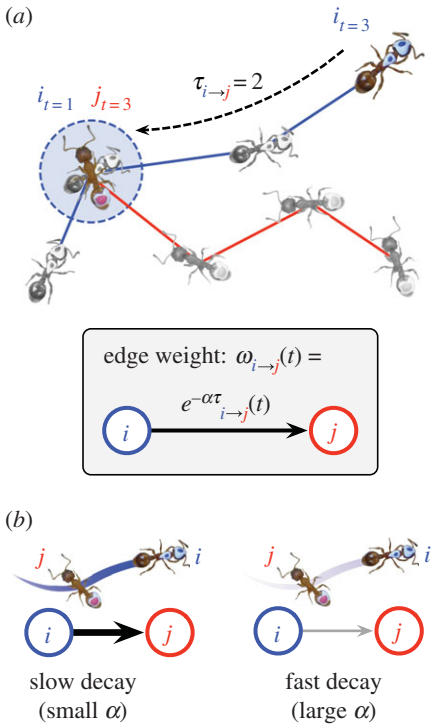

Figure 1. Inferring dynamic interaction networks from simultaneously-recorded spatial trajectories. (*a*) Methodology for calculating time-varying edge weights for the dynamic interaction networks. Ant *j* intersects a previously visited location of ant *i* at $t = 3$, leading to an intersect delay of $\tau_{i\to j}(3) = 2$ time-steps. Shaded circle represents the maximum transmission distance, which we consider to be half a body-length (1 mm). Edge weight is calculated using both the intersect delay $\tau_{i\to j}$ and intrinsic decay rate α of the spreading agent. (*b*) The weight of indirect interactions is modulated by the intrinsic decay rate of the transmitted agent.

Environmental decay rates of different real-world spreading agents can vary over many orders of magnitude; pheromone trails may fade away within a few minutes [33] or endure for several days [34], and similarly the off-host half-life of viral pathogens varies between a few minutes or hours [43] to hundreds of days [36]. Such huge natural variation raises the question of whether animal interaction networks are able to selectively modulate the dissemination of different agents with varying decay characteristics, and if so, how?

We sought to tackle these questions by applying our modelling framework to experimental data that we collected on the within-nest trajectories of individuals in 15 *Temnothorax albipennis* ant colonies (electronic supplementary material, §1.1). *Temnothorax albipennis* was chosen first because it is a recognized model social system in which high-fidelity tracking of individual spatial trajectories (necessary for the identification of spatial coincidence) is possible, and second because it is possible to perform controlled manipulations

of the society. By systematically varying the agent decay rate in the SI simulations, we obtained the predicted transmission properties of the ant networks for a range of different agents, from quickly decaying ephemeral agents that could only exploit direct interactions, to persistent agents that could additionally use weaker indirect pathways (figure 1*b*). Through comparison with null-model networks that control for spatial and temporal heterogeneity arising from the observed patterns of ant movement, we explored how the behaviour of individual ants generates the colony-level mixture of direct verses indirect interactions and how general network features support the overall transmission properties.

2. Results

2.1. Indirect pathways alter network transmission properties

To characterize the transmission of agents across the empirical ant networks, we performed approximately 300 million stochastic SI model simulations (electronic supplementary material, §1.3). Unlike classical SI models where the agent is characterized by a single infection probability p_s that represents the likelihood a direct interaction results in successful transmission [19,29,44,45], the potential for an agent to also be deposited in the environment required the additional specification of a decay rate α controlling the probability of indirect transmission (figure 1; Material and methods).

The importance of indirect pathways was confirmed by simulating the SI model over a range of p_s- and α-values to obtain the transmission parameter space for each colony (electronic supplementary material, figures S1–S2), and then comparing the parameter spaces of these more comprehensive networks with those of another *Temnothorax* study in which only CPIs were collected [4]. As standard CPI-based networks assume that agents never leave the host, the environmental decay rate α has no effect on transmission (figure 2*a*). However, when indirect transmission becomes possible, it plays a dominant role (figure 2*b*). This allows agents with very low infection probabilities to spread throughout an entire society if their decay rates are sufficiently low.

2.2. Spatial movement patterns enable transmission duality

Having shown that inclusion of indirect pathways strongly shape network transmission properties, we next attempted to understand how these properties are generated from the underlying ant movements within the nest. We compared the ant networks to an ensemble of networks generated by a spatial null-model in which the trajectories of individual ants possessed similar statistical properties to those observed, but which lacked the marked spatial fidelity exhibited by different individuals to different areas within the nest [6,46–48]. To generate a synthetic null-model trajectory from real ant data, each trajectory was permuted by randomly sampling from the observed step-length and turn-angle distributions (electronic supplementary material, figure S6). This ensured the absence of spatial fidelity in the synthetic trajectories, while other statistics were preserved. As the individual trajectories in this spatial null-model are effectively correlated random walks [49] (CRWs), we refer to these networks as such (Material and methods; electronic supplementary material, figures S5–S8 and §1.2.1).

For each colony, we ran SI simulations over the spatial null-model ensembles to extract their network transmission properties (figure 2*c*). These were then compared with that observed in the real colonies. The transmission parameter spaces of the observed ant networks exhibited a nonlinear transition from widespread to restricted infection as the agent decay rate α increased (figure 2*b*,*g*,*h*; electronic supplementary material, figures S1–S2 and Video S1). The close proximity of ants inside the nest means that the spread of an agent may not always be avoidable. We therefore compared the extent of spreading between the real and CRW networks to see if the ants' mobility patterns enhance or inhibit the transmission of different types of agent. Comparisons with the spatial null-model revealed a duality in the colony-level parameter spaces. Faster-than-expected spreading was observed for persistent (low-α) agents, and slower-than-expected spreading for short-lived (high-α) agents (figure 2*e*), although most colonies were dominated by inhibited spreading (electronic supplementary material, figures S1–S2).

To explore how the overall network topology emerges from the underlying spatial interactions, we considered a number of topological measures. It should be noted that the time-explicit nature of the networks we derive means that some measures commonly used to analyse networks must be considered in a time-varying context and in some cases new measures are required [29]. Two such measures include the pairwise interaction rate, and the mixture of (strong) direct and (weaker) indirect interactions between each ant pair. These capture fundamental aspects of the temporal interaction structure and are analogous to the degree distribution of a static network. In the context of an animal society, such measures can help identify how differences in the spatial fidelity of different individuals affect the frequency, type and distribution of interactions that occur between them. For example, an ant that shows fidelity to crowded areas such as the nest centre, will likely have a greater proportion of (strong) direct interactions compared with one that occupies the less crowded areas. Similarly, in species in which individuals show strong spatial fidelity, interactions with nearby neighbours will be dominated by physical contacts.

We began by examining the interaction rate statistics for individual ants (figure 3) and pairs of ants (electronic supplementary material, figures S9–S10). Compared to the spatial null-model, the 'real' ants accumulated approximately 1.75 times as many interactions (figure 3*a*), and their average intersect delays were 10–15% shorter (figure 3*c*). The co-occurrence of greater-than-expected interaction rates and the dominance of inhibited spreading over most $\{p_s,\alpha\}$ combinations (electronic supplementary material, figures S1–S2) may seem paradoxical; however, the interaction mixture was also strongly biased towards the weaker indirect interactions. Direct contacts were rare (mean = 1.05%, s.d. = 0.31%, range = 0.66–1.88%), occurring one-fifth less often than expected (figure 3*b*; electronic supplementary material, table S3). Therefore, although individual-level movement patterns elevate interaction rates, colonies reduce the occurrence of those events most likely to allow rapid spreading, i.e. direct interactions. This partially explains the dominance of spreading inhibition over most colonies transmission parameter spaces (see plots comparing

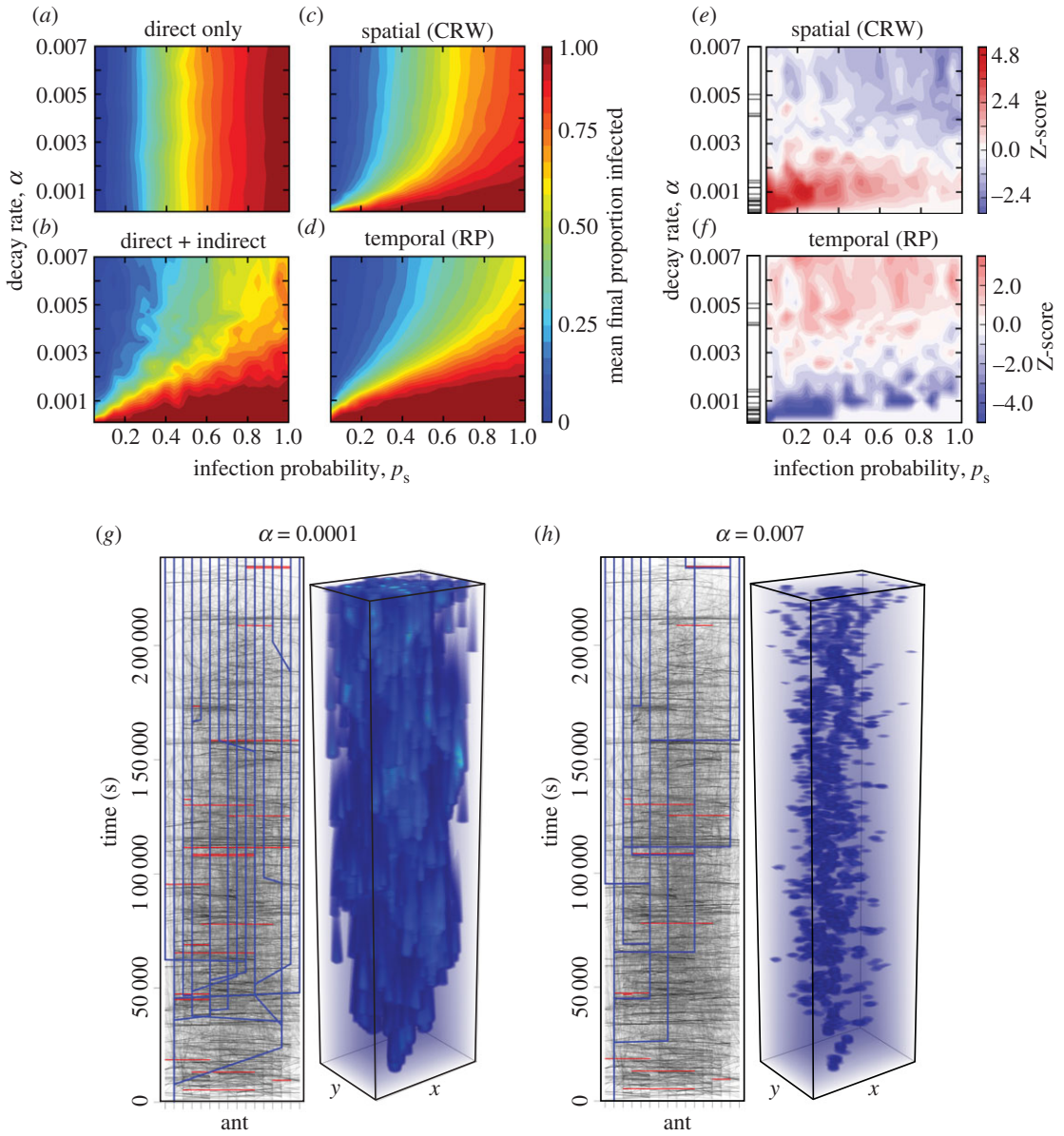

Figure 2. Spreading processes are influenced by ant interaction characteristics and environmental persistence of the agent. (*a–d*) Parameter space transmission plots for the SI model showing the final average proportion of infected ants for (*a*) interaction network from [4] composed purely of direct interactions, (*b*) interaction network for colony 15 where both direct and indirect interactions are present (see the electronic supplementary material, figures S1–S2 for other colonies), and interaction networks generated by the (*c*) spatial (CRW) and (*d*) temporal (RP) null-models. (*e,f*) Deviation between the observed and expected transmission for the (*e*) spatial and (*f*) temporal null-model networks as expressed by standardized *Z*-scores for colony 15 (blue and red regions indicate fewer or greater infected than expected, respectively). Leftmost rugplots show the distribution of ant pheromone decay rates obtained from the literature (see the electronic supplementary material, table S5 for further information). (*g,h*) The decay rate α determines the utilization of direct verses indirect pathways, and hence the eventual agent prevalence. In the time-ordered interaction networks (left panels), edge grey-scale is proportional to the intersect delay; darker indicates shorter delay, red indicates direct interaction. Blue lines trace the SI-simulated spread from a 'seed' ant. Three-dimensional boxes (right panels) show the spatial spreading of the agent within the nest. Blue areas indicate the kernel-smoothed infection intensity that captures the total integrated amount of infection contributed by all ants in the colony to that point and directly relates to the chance of transmission.

real with CRW networks in the electronic supplementary material, figures S1–S2).

To understand how the transmission duality arises, we calculated the network diameter as it provides a simple measure of the distance between individuals. The diameter is calculated as the longest of all shortest paths between every pair of individual within a network. Smaller diameters allow more rapid spreading because agents require fewer steps when travelling between any pair of individuals [50]. To assess whether the transmission duality can be explained by such a global property, we explored the variation of a weighted diameter measure (electronic supplementary material, §1.4) in both the real and CRW networks over a range of agent decay rates.

The decay-dependent transition between spreading inhibition and enhancement (figure 4*b*; electronic supplementary material, figures S1–S2) was found to directly correspond to the decay-dependent deviation of the observed and expected network diameters (figure 4*a*; electronic supplementary material, figure S3a). Most colonies showed clear decay-dependent diameter crossovers in which short-lived agents (high-α) are faced with longer-than-expected diameters. However, for increasingly persistent agents (decreasing α), the diameter progressively shortens until a crossover is reached

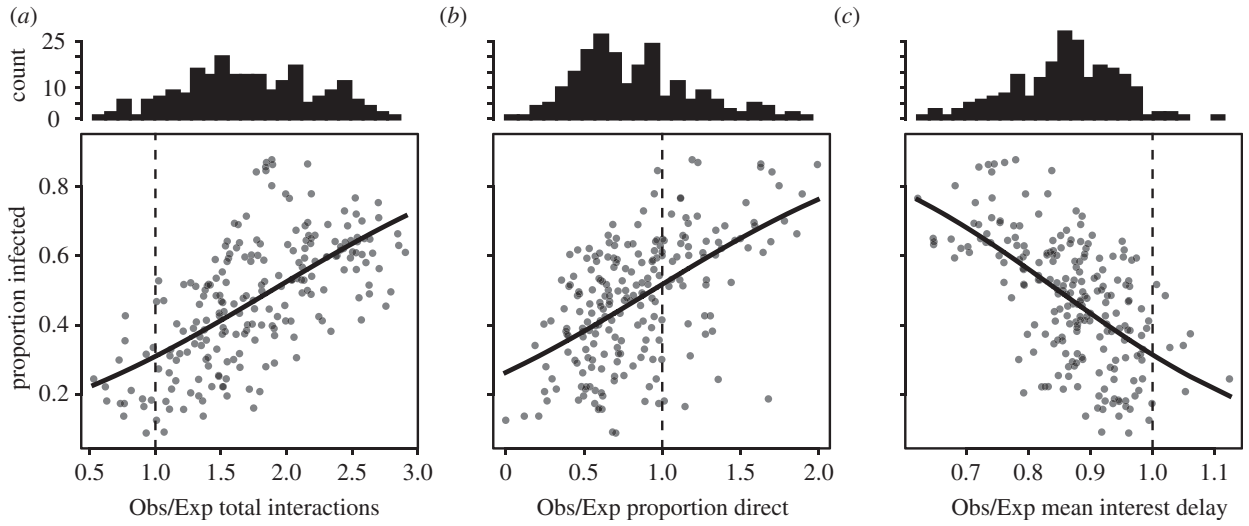

Figure 3. Spreading efficiency of individual ants depends upon the extent to which their interactions deviate from the spatial null-model expectation. Each point represents a single ant ($N = 216$). Data shown for an infection probability $p_s = 0.4$ and agent decay rate $\alpha = 0.001$. Solid lines show sigmoid (logistic) least-squares regressions (see the electronic supplementary material, table S3 for fit statistics). Marginal histograms show the distribution of the *x*-axis variable.

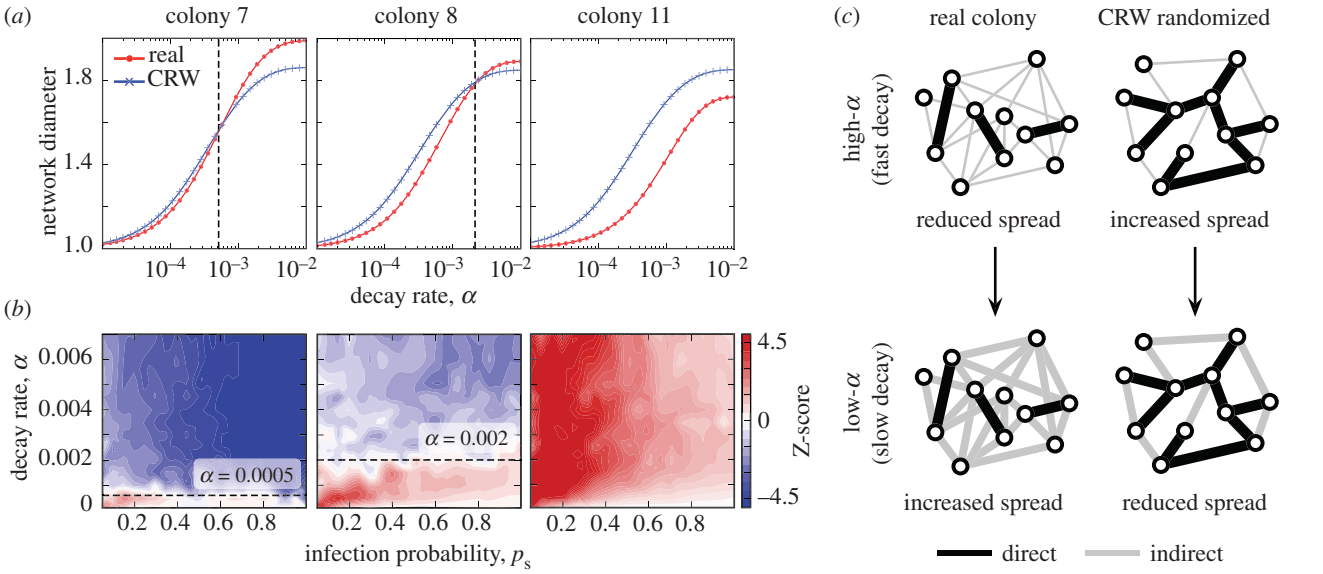

Figure 4. Mechanism for transmission duality. (*a*) Comparison of the network diameters for three colonies and their spatial (CRW) null-model networks for varying agent decay rate α. Dashed lines denotes the α-value at which a crossover in the diameters of the real and CRW networks occurs. (*b*) Parameter space transmission plots showing regions of enhanced (red) and inhibited (blue) spreading for the real colonies when compared to the CRW networks. Dashed lines correspond to the crossover points in (*a*). (*c*) Illustration of how differences in the total number of interactions, and the direct to indirect interaction bias can combine to produce transmission duality for varying decay rate α. Nodes represent individuals, black edges direct interactions and grey edges indirect interactions with line widths representative of their weight.

at which point it falls below that in the spatial null-model (figure 4*a*; electronic supplementary material, figure S3a).

The origin of this decay-dependence in the crossover between the diameters of the real and spatial null-model, could be explained by considering two variables known to influence the diameter: (i) the edge density which controls the number of alternative paths between pairs of individuals and (ii) the interaction mixture that modulates edge weights. Compared to the CRW networks, the real colonies had greater edge densities (figure 3*a*) and the interaction mixture was strongly biased towards indirect interactions (figure 3*b*). These features interact to produce the transmission duality in the following way (figure 4*c*): for rapidly decaying (high-α) agents, indirect links are much weaker relative to direct contacts, therefore although the high edge density has a diameter-reducing influence over all α-values, at high-α it is insufficient to counteract the diameter-raising effect of the bias towards indirect interactions. This leads to a larger-than-expected diameter (figure 4*a*) and hence spreading inhibition (figure 4*b*). Conversely, for slowly decaying agents (low-α), indirect link weights increase relative to direct contacts (Material and methods, equation (4.1)), rendering them viable for transmission. Thus, for persistent agents both features independently produce diameter-lowering effects in the ant networks, resulting in enhanced spreading.

2.3. Temporal activity patterns enable transmission duality

In addition to imperfect mixing in space, it has recently been shown that imperfect mixing in time also causes slower-than-expected transmission over time-ordered networks [44,51].

A well-known example is the non-Poissonian nature of human communications where activity is clustered into bursts with long inter-cluster intervals [52,53]. As ant activity patterns cover the full non-Poissonian spectrum from individual-level intermittency [54] to cyclical colony-level activity waves [55], we expected the ant interactions to exhibit non-Poissonian temporal statistics. To test this, we compared the ant networks to a set generated by the commonly used 'Randomly-Permuted (RP) times' temporal null-model [29] in which interaction time-stamps are randomly reshuffled among interactions on different edges (Material and methods; electronic supplementary material, §1.2.2 and figures S5, S7–S8). The distributions of the waiting times between repeated interactions on edges $\Delta t_{i\to j}$ showed the presence of clustering (a hallmark of non-Poissonian behaviour), which we quantified with the coefficient of variation $\mathrm{CV}^{\Delta t}_{i\to j}$ (see the electronic supplementary material, §1.5 and figure S8). Destruction of this feature in the RP networks resulted in enhanced spreading in most cases. Furthermore, the temporal organization of interactions in the ant networks produced another transmission duality, though the decay-dependence of the enhancement-inhibition was the opposite of that seen in the CRW networks. Transmission of persistent (low-α) agents was inhibited, while transmission of ephemeral agents was enhanced, but to a lesser extent (figure 2*f*; electronic supplementary material, figures S1–S2).

As with the CRW networks, the deviation between the real and RP network diameters to varying agent decay rates should be related to the transmission duality. However, because the time-aggregated representation of the RP networks are identical to the originals (the RP procedure conserves the total number of interactions, the interaction mixture and the intersect delay distribution on each edge; electronic supplementary material, figure S8), such topological features cannot explain the slightly reduced diameter of the RP networks at low-α (electronic supplementary material, figure S3b) or the corresponding low-α spreading inhibition (figure 2*f*; electronic supplementary material, figures S1–S2). These deviations must instead arise from differences in the temporal organization of events in the real and RP networks.

To understand how the temporal organization differs across these networks and how such differences generate a mechanism for transmission duality, we focused on the mean and variance of the waiting times between successive interactions on a given edge (electronic supplementary material, figure S8). The mean waiting time for a given edge $\overline{\Delta t}_{i\to j}$ acts like the edge density in the spatial duality mechanism; the shorter the mean delay, the greater the arrival-rate of opportunities for an agent to jump between individuals, and hence the lower the diameter. However, variation in the waiting time has the opposite effect; spreading is inhibited by 'bursty' waiting time distributions, i.e. those with long tails representing occasional extremely long intervals between interactions [52,53]. Therefore, in order for spreading to be enhanced, the ant networks should show either: (i) shorter-than-expected waiting times between events or (ii) lower-than-expected waiting time variation (burstiness), or both, with the converse applying for spreading inhibition. The ant networks showed both effects; 18% of the edges' $\overline{\Delta t}_{i\to j}$ were significantly different from the null expectation, of which 98% were shorter-than-expected (electronic supplementary material, figure S11), and 40% of edges' $\mathrm{CV}^{\Delta t}_{i\to j}$ were significant, of which 98% displayed more clustering than expected (electronic supplementary material, figure S12). However, these differences do not explain the decay-dependence of the transition (figure 2*f*).

The cause of the decay-dependence was found in the observation that α induces a bias in the interactions that the agent can use. Persistent agents can make use of all interaction types (low- to high-τ), but short-lived agents are limited to the smaller set of direct (low-τ) interactions. Because agents with differing decay rates are restricted to different sets of interactions, a decay-dependence can arise if the distribution of the waiting times between direct (or low-τ) interactions, is not equivalent to that between indirect (or high-τ) interactions.

We tested this conjecture by performed edge-thresholding [6]. An intersect delay threshold $\tau_{\max}$ was defined and all interactions with associated intersect delay greater than this were removed. Networks subjected to $\tau_{\max} = 0$ contained only direct edges, whereas higher $\tau_{\max}$ thresholds produced networks with a mixture of interaction strengths. All real and RP networks were thresholded over a range of $\tau_{\max}$ values and the mean waiting time for each edge and coefficient of variation calculated. Finally, both the observed values for these were expressed as a quotient of the mean expected values predicted by the RP networks. The edge-thresholding showed that both Obs/Exp $\overline{\Delta t}_{i\to j}$ and Obs/Exp $\mathrm{CV}^{\Delta t}_{i\to j}$ increase as $\tau_{\max}$ is raised (electronic supplementary material, figure S4). The enhanced spreading of ephemeral (high-α) agents compared to the temporal null-model expectation (figure 2*f*) is thus explained by the bias of such agents towards low-τ interactions, which have both shorter-than-expected waiting times and appear more regularly than expected.

2.4. Colony demographics govern spreading characteristics

A key benefit of using *T. albipennis* was the ability to perform controlled manipulative studies. Although the spatial and temporal null-models do provide a means to understand how the high-level properties emerge from the fine structuring of the interactions, it is also desirable to explore how underlying behavioural changes influence the interaction structure, and thereby also the high-level topological features. As raising a brood item from egg to eclosion requires both a substantial investment of time, energy and a considerable degree of coordination of the adult workers [1,46], we chose to manipulate the amount of brood across the colonies (electronic supplementary material, §1.1). This enabled us to alter the collective labour demands (e.g. feeding, grooming, etc.), and as the brood take up space within the nest, also influence the spatial distributions of direct and indirect interactions.

These manipulations revealed that colonies containing many brood had lower interaction rates (figure 5*a*), interaction mixtures biased towards weaker indirect interactions (figure 5*b*), and longer average delays between spatial coincidences (figure 5*c*). Such changes in network structure all contribute to reduced transmission efficiency (figure 5*d*). Moreover, as these factors together increase network diameter (figure 4*c*), the α crossover point between inhibited and enhanced spreading regimes also was also reduced (figure 5*e*). This leads to parameter space transmission plots for colonies with many brood being dominated by large regions of inhibited spreading, with only extremely slowly

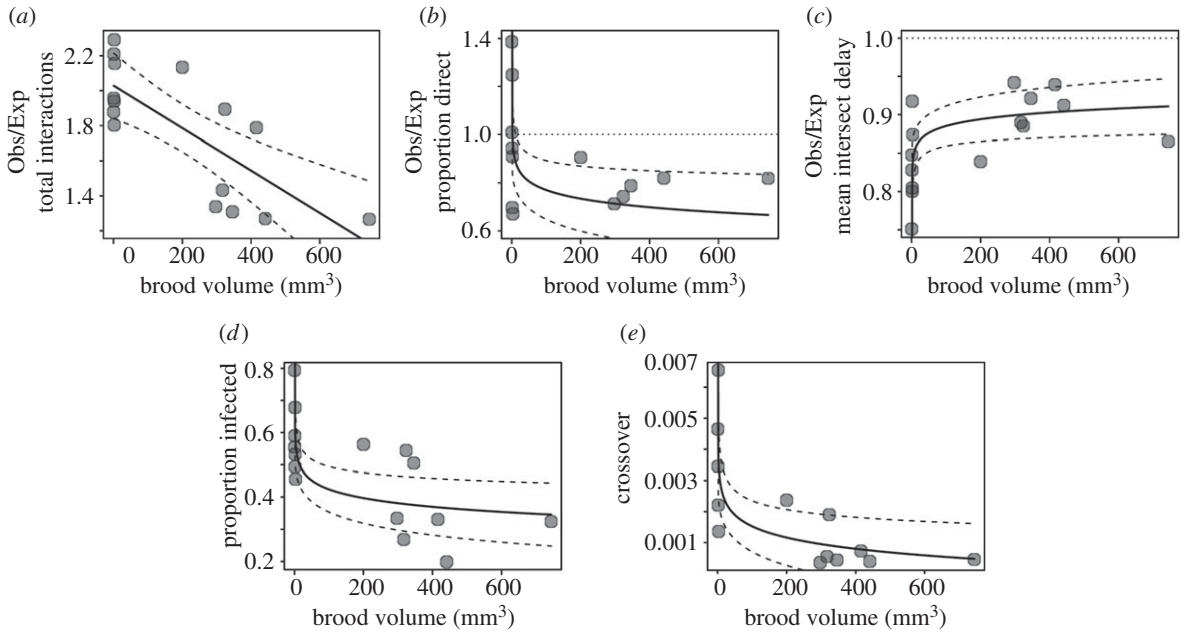

Figure 5. Experimental manipulation of colony brood demographics. Influence of brood volume on the structure of the interaction networks covering, (*a*) total combined count of indirect and direct interactions, (*b*) the proportion of direct interactions and (*c*) average intersect delay, as well as spreading characteristics such as (*d*) the proportion of infected individuals and (*e*) the α-value of the duality crossover. Each point represents the mean for a single colony ($N = 15$). Solid lines represent least-squares fits, dashed lines denote the 95% CI (see the electronic supplementary material, table S2 for fit statistics). All observed to expected ratios (Obs/Exp), and diameter crossovers are made by comparison with the spatial null-model.

decaying agents subject to enhanced spread (electronic supplementary material, figures S1–S2). This demonstrates that, by inducing changes in the fine structure of the interaction network, individual-level behaviour can affect overall transmission properties.

There is no reason to assume that the reduced interaction rate in the presence of many brood originates from workers actively avoiding interactions. A more parsimonious explanation is that it is a consequence of the task-demands associated with the brood. For example, a greater number of brood requires that workers spend more time caring for brood items. As the brood are stationary, the overall worker movement rate is reduced, which reduces the rate that workers encounter one another. Indeed, 'slow' colonies (defined by the mean duration individuals spent standing still—the 'stop duration') had interaction mixtures that were biased away from the strong direct interactions, towards the weaker indirect interactions. Although this relationship was on the border of statistical significance (electronic supplementary material, table S2), it supports theoretical predictions that low movement rates should inhibit spreading in animal societies [14].

3. Discussion

From the pheromone trails of army ants [8] and the honey pots of bumblebees [12], to the symbolic cave paintings of early humans or the graffiti of today, indirect exchange of material or information is pervasive throughout the animal kingdom. Yet the recent interest in spreading processes over human [17–21] and animal [3,4,6,13,23–26,28] contact networks has neglected this important pathway.

Perhaps our most striking finding was that a single interaction network in which interactions follow a precise ordering in time, and are physically embedded in space, is able to either enhance or inhibit spreading, depending upon the environmental decay characteristics of the agent in question. It should be emphasized that this duality is not a contradiction in terms: a given network may only either enhance *or* inhibit an agent with a given environmental persistence. Clearly claims about the presence of such phenomena are dependent upon the nature of the null-model chosen for network comparisons. Therefore, as the ant networks possessed both spatial and temporal dimensions, we considered two. The first was with a null-model in which the observed movement patterns of individual ants were permuted to produce an ensemble of unbiased 'random' trajectories (electronic supplementary material, figures S5 and S8). Because interactions between random walks are random, the distribution of interactions in time and space is also random with respect to the physical constraints imposed by the nest. Hence, these synthetic trajectories represented our primary null-model. The second comparison was with a 'legacy' temporal 'RP times' null-model (see [29] and references therein) that shuffles the timing of interactions (electronic supplementary material, figure S8), but which does not preserve associated features within the spatial domain, such as the requirement for biologically reasonable trajectories underlying the interaction timings (electronic supplementary material, figure S5). The temporal null-model fails to preserve the spatial characteristics of the interactions because, as it consists of a simple permutation of the event-ordering, it introduces randomness at a higher organizational level—that of the network. This differs from the spatial null-model, which operates at a more fundamental level—that of individual trajectories. Although it may be possible to conceive of a more sophisticated temporal null-model that not only destroys non-random structures in the time domain (which the RP procedure succeeds in doing), but also represents the result of interactions between a set of agents walking along realistic spatial trajectories (which it does not), it is a non-trivial challenge and beyond the scope of the present

study. Nevertheless, the use of the temporal RP null-model allows a clear separation of the effects of non-random ordering of interactions in time and non-random distributions of interactions arising solely from spatial constraints.

It is tempting to suggest that the strong duality originating from the ants' spatial fidelity may represent a strategy to enhance persistent-but-beneficial agents (e.g. home-range pheromones with low evaporation rates [56]) whilst inhibiting ephemeral-but-harmful agents (e.g. virulent pathogens with short off-host half-lives [30]). However, as pathogen decay rates are also likely to be under strong selection, it could equally be the case that many harmful agents exploit the enhanced spreading for persistent agents. To resolve this question, we searched the literature for estimates of the environmental persistence of agents known to circulate on social insect interaction networks, namely ant pheromones and pathogens (electronic supplementary material, table S5). This resulted in a wealth of decay rates for pheromones, but did not reveal any off-host decay rates (or half-life durations, from which the decay rate can be obtained) for pathogens. Overall, pheromone decay rates were highly skewed towards low α-values, and as the ants' movement patterns enhance the transmission of such agents (figure 2*e*), we expect that individual spatial fidelity should enhance the dissemination of information carried by persistent pheromones.

While it has been shown that ants can acquire the spores of at least two species of pathogenic fungi simply by walking over contaminated surfaces, and that they sometimes die from doing so [57], it seems likely that the absence of off-host decay rates for such agents is due to the absence of studies searching for pathogens that use indirect transmission. Nevertheless, there has been some progress towards a more comprehensive understanding of the role of environmental persistence, at least for pathogens that represent direct threats to human health, e.g. avian influenza [36,38], or agriculturally important species such as cattle [23,58], deer [40] and honeybees [59–64]. Therefore, until quantitative data on the environmental persistence of social insect pathogens becomes available, we refrain from further speculation on the extent to which their interaction networks do function to balance the transmission of beneficial materials and information against the transmission of disease.

Despite the limited quantitative decay rate estimates for different classes of real-world agents, it is still possible to make quantitative inferences about the extent to which the observed interaction patterns could potentially balance the benefits associated with transmission of a 'good' agent, against the costs associated with transmission of a 'bad' agent. The simplest means of doing so is to assume the presence of two different agents, each with its own spreading characteristics (p_s, α), but now also with a given 'utility'. This measures the extent to which the agent benefits the ant society or is detrimental to it. If the spread of the agents are independent of one another, then the transmission plot shown in figure 2*b* provides the fraction of the population that will be infected by each agent. Combining this fraction with the utility of the agent, it is possible to calculate the net cost or benefit associated for the pair of agents (see the electronic supplementary material, S1, §1.8 and figure S13 for a detailed explanation of how utility values of each agent can be incorporated into such analyses).

As the networks we have studied are generated from the movement of individuals living in a society, it is appropriate to consider how generalizable our results will be to other animal societies. Research is beginning to reveal that there are generic statistical features underlying the spatial and temporal mobility patterns of individuals exhibiting some fidelity to a central-place, be it a social insect nest, or a human city. One such feature is spatial recursion, which originates from the fact that individuals living in a complex society, regularly travel to and from one or several locations of interest, such as foraging grounds (e.g. restaurants), resting areas (e.g. home) and work areas (e.g. schools, offices). Recursive behaviour has been described in several ant species [6,46,65], and also in a range of species that are only distantly related to ants, including honeybees [66], bumblebees [47], wasps [48], amphibians [67], canids [68], ungulates [69,70], non-human primates [71–73] and humans [22,71,74,75]. Another generic statistical property common to a diverse range of animal species is temporal intermittency. For example, in humans, communication patterns, individual activity and movement show 'bursty' dynamics that are clustered in time [44]. We find that interactions in *T. albipennis* are also bursty (electronic supplementary material, figures S7 and S10). Therefore, because these spatial and temporal features of individual movement are seen across a diverse range of systems, it is natural to predict that the generalities (but not the specifics) of our results might also be expected in other animal societies.

In addition to the 'same-place, same-time' and 'same-place, different-time' interactions considered here, a third class of interaction can also be defined, namely 'different-place, different-time' interactions. This category describes cases where there is a time lag between signal emission and receipt, and where the location of the sender at the time of sending is different to the location of the receiver at the time of receipt. Alarm signalling and nest evacuation in social insects fall into this category, as they are mediated by volatile pheromones that are broadcast into the air by the sender [1]. For most social insect examples, both the time-delay between signal emission and detection, and the distances between sender and receiver, are often short. However, the viability of this interaction type for distant transmission can change based on the medium in which the society lives. In aquatic environments where currents and advective flows are common, an agent that is secreted into the environment by a sender at one location will form thin filaments extending downstream of the source. These may then be detected by a far-removed receiver [76]. In such cases, one might expect fewer same-place, same time interactions, and more different-place, different-time interactions, simply because the presence of an advective flow avoids the need to spend energy locating and contacting a conspecific.

In this work, we assumed that transmission of an agent would not disrupt the ants' existing behaviour. This is not always the case, with many group-living animals having evolved sophisticated sensory mechanisms to detect the presence of both beneficial and harmful agents, and modify their behaviour accordingly. Examples of detection and active responses to beneficial substances (e.g. food, nest-mate pheromones, etc.) are well known [8,33], but active responses by susceptible individuals to the presence of harmful agents have received less attention [77]. In non-eusocial animal groups where the unit of selection is the individual, susceptible individuals often avoid the infected individuals [77,78], but in eusocial species such as the ants where the unit of selection is the colony, infected individuals can commit altruistic suicide by abandoning the colony, thus

avoiding further contamination of the colony [79]. As we show through our experimental manipulations, modifications of individual behaviour can significantly alter the high-level structural features of the interaction networks, and so influence their efficiency at disseminating different types of agent. Although the focus here was on studying real ant colonies, an interesting future direction would be to use spatially and temporally explicit agent-based models to theoretically investigate how different individual-level movement rules, and how interindividual variation in those movement rules, translates into the structural features of the overall interaction networks. The major advantage of working at the level of behavioural traits would be in the ability to investigate how individual behaviours—and interindividual variation—influences overall network properties, whilst simultaneously imposing a variety of different constraints upon the agents themselves, something that is impossible with permutation-based approaches. Such constraints are incredibly difficult to integrate into permutation-based approaches that work at a higher level, such as the interaction networks themselves, to randomize various statistical properties.

To summarize, our framework provides a foundation to better understand how the transmission processes that occur across animal populations might emerge from the multitude of different interaction types within them. Such a foundation is essential if we are to better understand how group members might modulate their behaviours to influence the overall properties of the society to which they belong.

4. Material and methods

4.1. Empirically derived interaction networks

We extracted two-dimensional spatial trajectories of ants as they moved within the nest by exploiting the flat nest geometry and individually tagging colony members (electronic supplementary material, §1). For each of the 15 colonies, time-ordered networks were derived from the experimental spatial data by considering path crossings as weighted directional edges. An edge from ant $i \to j$ was present at time t, if ant j was found at a location previously visited by ant i. The edge weight was defined as a monotonically decaying function of the elapsed time since i's most recent visit, $\tau_{i\to j}(t)$ (figure 1*a*). The edge weight was set such that direct interactions were assigned a maximal weight of 1, and indirect spatial coincidences assigned weaker weights modulated by the intersect delay. The decay was given an exponential form and parametrized by a decay rate, α [56]. Specifically, the weight of an edge $i \to j$ at time t was calculated as

$$\omega_{i\to j}(t) = \mathrm{e}^{-\alpha\tau_{i\to j}(t)}. \tag{4.1}$$

If at time t ant j was not at one of i's previously visited locations, and if i and j were not in physical contact, then $\omega_{i\to j}(t) = 0$ (i.e. no edge was present).

4.2. Susceptible-Infected model

To simulate agent dissemination over these networks, we used an SI model parametrized by a transition probability p_s that was further modulated by the time-varying edge weights described above. At each time point and for all pairs of ants, possible spreading from ant $i \to j$ at time t occurred with probability

$$\Pr(j \to I, t) = \begin{cases} p_s\ \omega_{i\to j}(t), & \text{if } X(i, t - \omega_{i\to j}(t)) = I, \\ 0, & \text{otherwise.} \end{cases} \tag{4.2}$$

Here, $X(i, t)$ is the state of ant i at time t (either S = Susceptible or I = Infected), which allowed us to ensure that the transmission pathways respected the time-ordering, i.e. transmission was only possible if the sender was infected when historically at the location (electronic supplementary material, §1). For each simulation run, a single ant was defined as the initially infected 'seed' and all others were designated as susceptible. For each $\{p_s, \alpha\}$ combination, the full range of initial conditions was exhausted by successively designating each ant as the seed. Computational simulation of this process was performed by translating this description into an evolving dynamical network [80,81] and simulating using the NetEvo software library [82] (http://www.netevo.org).

4.3. Null-models

The spreading characteristics of the real ant colonies were compared with that of a spatial and a temporal null-model. For the spatial null-model, each individual trajectory was compared with a null trajectory ensemble of CRWs, generated by re-sampling from the observed step-length and turn-angle distributions (electronic supplementary material, figure S6). This re-sampling ensured the absence of spatial fidelity in the synthetic trajectories, while the other statistics present in the original trajectory were preserved. For the temporal null-model, we used the RP times technique [29] to remove temporal clustering of interactions on edges. The interaction event times on each edge were randomly shuffled, while ensuring that the count of interactions on that edge remained constant (electronic supplementary material, figure S8).

Data accessibility. Datasets used in this study are provided as the electronic supplementary material.

Authors' contributions. Both authors contributed equally to this work. T.O.R. and T.E.G. conceived and designed the study, T.O.R. collected and processed the spatial ant data, T.E.G. developed the model and ran the computational simulations, T.O.R. and T.E.G. analysed the data and wrote the manuscript.

Competing interests. We declare we have no competing interests.

Funding. This work was supported by EU Marie Curie Actions Fellowship, 'Mapping spatial interaction networks in honeybee colonies', project number 30114 (T.O.R.) and EPSRC grant no. EP/E501214/1 (T.E.G.).

Acknowledgements. T.O.R. thanks Ana Sendova-Franks and Nigel Franks for provision of experimental facilities. Simulations and analyses were carried out using the computational facilities of the Advanced Computing Research Centre, University of Bristol and UNIL VitalIT.

References

1. Hölldobler B, Wilson EO. 1990 *The ants*. Cambridge, MA: Harvard University Press.
2. Greene MJ, Gordon DM. 2007 Interaction rate informs harvester ant task decisions. *Behav. Ecol.* **18**, 451–455. (doi:10.1093/beheco/arl105)
3. Sendova-Franks AB, Hayward RK, Wulf B, Klimek T, James R, Planqué R, Britton NF, Franks NR. 2010 Emergency networking: famine relief in ant colonies. *Anim. Behav.* **79**, 473–485. (doi:10.1016/j.anbehav.2009.11.035)
4. Blonder B, Dornhaus A. 2011 Time-ordered networks reveal limitations to information flow in ant colonies. *PLoS ONE* **6**, e20298. (doi:10.1371/journal.pone.0020298)
5. Pinter-Wollman N, Wollman R, Guetz A, Holmes S, Gordon DM. 2011 The effect of individual variation on the structure and function of interaction networks in harvester ants. *J. R. Soc. Interface* **8**, 1562–1573. (doi:10.1098/rsif.2011.0059)
6. Mersch DP, Crespi A, Keller L. 2013 Tracking individuals shows spatial fidelity is a key regulator

of ant social organization. *Science* **340**, 1090–1093. (doi:10.1126/science.1234316)

7. Razin N, Eckmann JP, Feinerman O. 2013 Desert ants achieve reliable recruitment across noisy interactions. *J. R. Soc. Interface* **10**, 20130079. (doi:10.1098/rsif.2013.0079)
8. Schneirla T. 1934 Raiding and other outstanding phenomena in the behavior of army ants. *Proc. Natl Acad. Sci. USA* **20**, 316–321. (doi:10.1073/pnas.20.5.316)
9. Grassé PP. 1959 La reconstruction du nid et les coordinations interindividuelles chez *Belli-cositermes natalensis* et *Cubitermes* sp. la théorie de la stigmergie: Essai d'interprétation du comportement des termites constructeurs. *Insectes Sociaux* **6**, 41–80. (doi:10.1007/BF02223791)
10. Greene MJ, Gordon DM. 2003 Social insects: cuticular hydrocarbons inform task decisions. *Nature* **423**, 32. (doi:10.1038/423032a)
11. Hart AG, Ratnieks FL. 2001 Leaf caching in the leafcutting ant *Atta colombica*: organizational shift, task partitioning and making the best of a bad job. *Anim. Behav.* **62**, 227–234. (doi:10.1006/anbe.2001.1743)
12. Dornhaus A, Chittka L. 2005 Bumble bees (*Bombus terrestris*) store both food and information in honeypots. *Behav. Ecol.* **16**, 661–666. (doi:10.1093/beheco/ari040)
13. Naug D. 2008 Structure of the social network and its influence on transmission dynamics in a honeybee colony. *Behav. Ecol. Sociobiol.* **62**, 1719–1725. (doi:10.1007/s00265-008-0600-x)
14. Naug D, Camazine S. 2002 The role of colony organization on pathogen transmission in social insects. *J. Theoret. Biol.* **215**, 427–439. (doi:10.1006/jtbi.2001.2524)
15. Cremer S, Armitage SA, Schmid-Hempel P. 2007 Social immunity. *Curr. Biol.* **17**, R693–R702. (doi:10.1016/j.cub.2007.06.008)
16. Stroeymeyt N, Casillas-Pérez B, Cremer S. 2014 Organisational immunity in social insects. *Curr. Opinion Insect Sci.* **5**, 1–15. (doi:10.1016/j.cois.2014.09.001)
17. Lloyd-Smith JO, Schreiber SJ, Kopp PE, Getz WM. 2005 Superspreading and the effect of individual variation on disease emergence. *Nature* **438**, 355–359. (doi:10.1038/nature04153)
18. Eagle N, Pentland AS, Lazer D. 2009 Inferring friendship network structure by using mobile phone data. *Proc. Natl Acad. Sci. USA* **106**, 15 274–15 278. (doi:10.1073/pnas.0900282106)
19. Salathé M, Kazandjieva M, Lee JW, Levis P, Feldman MW, Jones JH. 2010 A high-resolution human contact network for infectious disease transmission. *Proc. Natl Acad. Sci. USA* **107**, 22 020–22 025. (doi:10.1073/pnas.1009094108)
20. Stehlé J *et al.* 2011 High-resolution measurements of face-to-face contact patterns in a primary school. *PLoS ONE* **6**, e23176. (doi:10.1371/journal.pone.0023176)
21. Isella L, Stehlé J, Barrat A, Cattuto C, Pinton JF, Van den Broeck W. 2011 What's in a crowd? Analysis of face-to-face behavioral networks. *J. Theoret. Biol.* **271**, 166–180. (doi:10.1016/j.jtbi.2010.11.033)
22. Sun L, Axhausen KW, Lee DH, Huang X. 2013 Understanding metropolitan patterns of daily encounters. *Proc. Natl Acad. Sci. USA* **110**, 13 774–13 779. (doi:10.1073/pnas.1306440110)
23. Bohm M, Hutchings MR, Whiteplain PCL. 2009 Contact networks in a wildlife-livestock host community: identifying high-risk individuals in the transmission of bovine TB among badgers and cattle. *PLoS ONE* **4**, e5016. (doi:10.1371/journal.pone.0005016)
24. Rushmore J, Caillaud D, Matamba L, Stumpf RM, Borgatti SP, Altizer S. 2013 Social network analysis of wild chimpanzees provides insights for predicting infectious disease risk. *J. Anim. Ecol.* **82**, 976–986. (doi:10.1111/1365-2656.12088)
25. Chen S, White BJ, Sanderson MW, Amrine DE, Ilany A, Lanzas C. 2014 Highly dynamic animal contact network and implications on disease transmission. *Sci. Rep.* **4**, 4472. (doi:10.1038/srep04472)
26. Aiello C, Nussear K, Walde A, Esque T, Emblidge P, Sah P, Bansal S, Hudson PJ. 2014 Disease dynamics during wildlife translocations: disruptions to the host population and potential consequences for transmission in desert tortoise contact networks. *Anim. Conserv.* **17**, 27–39. (doi:10.1111/acv.12147)
27. Otterstatter MC, Thomson JD. 2007 Contact networks and transmission of an intestinal pathogen in bumble bee (*Bombus impatiens*) colonies. *Oecologia* **154**, 411–421. (doi:10.1007/s00442-007-0834-8)
28. Jeanson R. 2012 Long-term dynamics in proximity networks in ants. Anim. Behav. **83**, 915–923. (doi:10.1016/j.anbehav.2012.01.009)
29. Holme P, Saramäki J. 2012 Temporal networks. *Phys. Rep.* **519**, 97–125. (doi:10.1016/j.physrep.2012.03.001)
30. Walther BA, Ewald PW. 2004 Pathogen survival in the external environment and the evolution of virulence. *Biol. Rev.* **79**, 849–869. (doi:10.1017/S1464793104006475)
31. Godfrey SS, Bull CM, James R, Murray K. 2009 Network structure and parasite transmission in a group living lizard, the gidgee skink, *Egernia stokesii*. *Behav. Ecol. Sociobiol.* **63**, 1045–1056. (doi:10.1007/s00265-009-0730-9)
32. Crandall DJ, Backstromb L, Cosley D, Surib S, Huttenlocher D, Kleinberg J. 2010 Inferring social ties from geographic coincidences. *Proc. Natl Acad. Sci. USA* **107**, 22 436–22 441. (doi:10.1073/pnas.1006155107)
33. Wilson EO. 1962 Chemical communication among workers of the fire ant *Solenopsis saevissima* (Fr. Smith) 1. The Organization of Mass-Foraging. *Anim. Behav.* **10**, 134–147. (doi:10.1016/0003-3472(62)90141-0)
34. Moser JC, Blum MS. 1963 Trail marking substance of the Texas leaf-cutting ant: source and potency. *Science* **140**, 1228–1231. (doi:10.1126/science.140.3572.1228)
35. Edelstein-Keshet L, Watmough J, Ermentrout GB. 1995 Trail following in ants: individual properties determine population behaviour. *Behav. Ecol. Sociobiol.* **36**, 119–133. (doi:10.1007/BF00170717)
36. Breban R, Drake JM, Stallknecht DE, Rohani P. 2009 The role of environmental transmission in recurrent avian influenza epidemics. *PLoS Comput. Biol.* **5**, e1000346. (doi:10.1371/journal.pcbi.1000346)
37. Xiao Y, French NP, Bowers RG, Clancy D. 2007 Pair approximations and the inclusion of indirect transmission: theory and application to between farm transmission of *Salmonella*. *J. Theoret. Biol.* **244**, 532–540. (doi:10.1016/j.jtbi.2006.08.019)
38. Rohani P, Breban R, Stallknecht DE, Drake JM. 2009 Environmental transmission of low pathogenicity avian influenza viruses and its implications for pathogen invasion. *Proc. Natl Acad. Sci. USA* **106**, 10 365–10 369. (doi:10.1073/pnas.0809026106)
39. Roche B, Drake JM, Rohani P. 2011 The curse of the Pharaoh revisited: evolutionary bi-stability in environmentally transmitted pathogens. *Ecol. Lett.* **14**, 569–575. (doi:10.1111/j.1461-0248.2011.01619.x)
40. Almberg ES, Cross PC, Johnson CJ, Heisey DM, Richards BJ. 2011 Modeling routes of chronic wasting disease transmission: environmental prion persistence promotes deer population decline and extinction. *PLoS ONE* **6**, e19896. (doi:10.1371/journal.pone.0019896)
41. VanderWaal KL, Atwill ER, Isbell L, McCowan B. 2014 Linking social and pathogen transmission networks using microbial genetics in giraffe (*Giraffa camelopardalis*). *J. Anim. Ecol.* **83**, 406–414. (doi:10.1111/1365-2656.12137)
42. Hethcote H. 2000 The mathematics of infectious diseases. *SIAM Rev.* **42**, 599–653. (doi:10.1137/S0036144500371907)
43. Stephenson EH, Larson EW, Dominik JW. 1984 Effect of environmental factors on aerosol-induced lassa virus infection. *J. Med. Virol.* **14**, 295–303. (doi:10.1002/jmv.1890140402)
44. Karsai M, Kivelä M, Pan RK, Kaski K, Kertész J, Barabási AL, Saramäki J. 2011 Small but slow world: How network topology and burstiness slow down spreading. *Phys. Rev. E* **83**, 025102(R). (doi:10.1103/PhysRevE.83.025102)
45. Stehlé J *et al.* 2011 Simulation of an SEIR infectious disease model on the dynamic contact network of conference attendees. *BMC Med.* **9**, 1–87. (doi:10.1186/1741-7015-9-87)
46. Sendova-Franks AB, Franks NR. 1995 Spatial relationships within nests of the ant *Leptothorax unifasciatus* (Latr.) and their implications for the division of labour. *Anim. Behav.* **50**, 121–136. (doi:10.1006/anbe.1995.0226)
47. Jandt JM, Dornhaus A. 2009 Spatial organization and division of labour in the bumblebee *Bombus impatiens*. *Anim. Behav.* **77**, 641–651. (doi:10.1016/j.anbehav.2008.11.019)
48. Baracchi D, Zaccaroni M, Cervo R, Turillazzi S. 2010 Home range analysis in the study of spatial organization on the comb in the paper wasp *Polistes dominulus*. *Ethology* **116**, 579–587.
49. Kareiva PM, Shigesada N. 1983 Analyzing insect movement as a correlated random walk. *Oecologia* **56**, 234–238. (doi:10.1007/BF00379695)
50. Boccaletti S, Latora V, Moreno Y, Chavez M, Hwang DU. 2006 Complex networks: structure and

dynamics. *Phys. Rep*. **424**, 175–308. (doi:10.1016/j.physrep.2005.10.009)

51. Yang Z, Cui AX, Zhou T. 2011 Impact of heterogeneous human activities on epidemic spreading. *Physica A* **390**, 4543–4548. (doi:10.1016/j.physa.2011.06.068)
52. Barabási AL. 2005 The origin of bursts and heavy tails in humans dynamics. *Nature* **435**, 207–212. (doi:10.1038/nature03459)
53. Goh KI, Barabási AL. 2008 Burstiness and memory in complex systems. *Europhys. Lett*. **81**, 48002. (doi:10.1209/0295-5075/81/48002)
54. Cole BJ. 1991 Is animal behaviour chaotic? Evidence from the activity of ants. *Proc. R. Soc. Lond. B* **244**, 253–259. (doi:10.1098/rspb.1991.0079)
55. Boi S, Couzin I, Del Buono N, Franks N, Britton N. 1999 Coupled oscillators and activity waves in ant colonies. *Proc. R. Soc. Lond. B* **266**, 371–378. (doi:10.1098/rspb.1999.0647)
56. Jeanson R, Ratnieks FL, Deneubourg JL. 2003 Pheromone trail decay rates on different substrates in the Pharaoh's ant, *Monomorium pharaonis*. *Physiol. Entomol*. **28**, 192–198. (doi:10.1046/j.1365-3032.2003.00332.x)
57. Brutsch T, Felden A, Reber A, Chapuisat M. 2014 Ant queens (Hymenoptera: Formicidae) are attracted to fungal pathogens during the initial stage of colony founding. *Myrmecol. News* **20**, 71–76.
58. Woodroffe R *et al.* 2006 Culling and cattle controls influence tuberculosis risk for badgers. *Proc. Natl Acad. Sci. USA* **103**, 14 713–14 717. (doi:10.1073/pnas.0606251103)
59. Bailey L, Ball BV. 1991 *Honey bee pathology*. New York, NY: Academic Press.
60. De Guzman LI, Rinderer TE, Beaman LD. 1993 Survival of *Varroa jacobsoni* Oud.(Acari: Varroidae) away from its living host *Apis mellifera* L. *Exp. Appl. Acarol*. **17**, 283–290. (doi:10.1007/BF02337278)
61. Durrer S, Schmid-Hempel P. 1994 Shared use of flowers leads to horizontal pathogen transmission. *Proc. R. Soc. Lond. B* **258**, 299–302. (doi:10.1098/rspb.1994.0176)
62. Schwarz HH, Huck K. 1997 Phoretic mites use flowers to transfer between foraging bumblebees. *Insectes Sociaux* **44**, 303–310. (doi:10.1007/s000400050051)
63. Chen Y, Evans JD, Smith IB, Pettis JS. 2008 *Nosema ceranae* is a long-present and wide-spread microsporidian infection of the European honey bee (*Apis mellifera*) in the United States. *J. Invert. Pathol*. **97**, 186–188. (doi:10.1016/j.jip.2007.07.010)
64. Singh R *et al.* 2010 RNA viruses in hymenopteran pollinators: evidence of inter-taxa virus transmission via pollen and potential impact on non-Apis hymenopteran species. *PLoS ONE* **5**, e14357. (doi:10.1371/journal.pone.0014357)
65. Beverly BD, McLendon H, Nacu S, Holmes S, Gordon DM. 2009 How site fidelity leads to individual differences in the foraging activity of harvester ants. *Behav. Ecol*. **20**, 633–638. (doi:10.1093/beheco/arp041)
66. Baracchi D, Cini A. 2014 A socio-spatial combined approach confirms a highly compartmentalized structure in honeybees. *Ethology* **120**, 1167–1176. (doi:10.1111/eth.12290)
67. Schwarzkopf L, Alford RA. 2002 Nomadic movement in tropical toads. *Oikos* **96**, 492–506. (doi:10.1034/j.1600-0706.2002.960311.x)
68. Giuggioli L, Potts JR, Harris S. 2011 Animal interactions and the emergence of territoriality. *PLoS Comput. Biol*. **7**, e1002008. (doi:10.1371/journal.pcbi.1002008)
69. Bar-David S, Bar-David I, Cross PC, Ryan SJ, Knechtel CU, Getz WM. 2009 Methods for assessing movement path recursion with application to African buffalo in South Africa. *Ecology* **90**, 2467–2479. (doi:10.1890/08-1532.1)
70. Benhamou S, Riotte-Lambert L. 2012 Beyond the Utilization Distribution: identifying home range areas that are intensively exploited or repeatedly visited. *Ecol. Model*. **227**, 112–116. (doi:10.1016/j.ecolmodel.2011.12.015)
71. Boyer D, Crofoot MC, Walsh PD. 2012 Non-random walks in monkeys and humans. *J. R. Soc. Interface* **9**, 842–847. (doi:10.1098/rsif.2011.0582)
72. Boyer D, Solis-Salas C. 2014 Random walks with preferential relocations to places visited in the past and their application to biology. *Phys. Rev. Lett*. **112**, 240601. (doi:10.1103/PhysRevLett.112.240601)
73. Schreier AL, Grove M. 2014 Recurrent patterning in the daily foraging routes of hamadryas baboons (*Papio hamadryas*): spatial memory in large-scale versus small-scale space. *Amer. J. Primatol*. **76**, 421–435. (doi:10.1002/ajp.22192)
74. Gonzalez MC, Hidalgo CA, Barabasi AL. 2008 Understanding individual human mobility patterns. *Nature* **453**, 779–782. (doi:10.1038/nature06958)
75. Song C, Koren T, Wang P, Barabási AL. 2010 Modelling the scaling properties of human mobility. *Nat. Phys*. **6**, 818–823. (doi:10.1038/nphys1760)
76. Torney C, Neufeld Z, Couzin ID. 2009 Context-dependent interaction leads to emergent search behavior in social aggregates. *Proc. Natl Acad. Sci. USA* **106**, 22 055–22 060. (doi:10.1073/pnas.0907929106)
77. Funk S, Gilad E, Watkins C, Jansen VA. 2009 The spread of awareness and its impact on epidemic outbreaks. *Proc. Natl Acad. Sci. USA* **106**, 6872–6877. (doi:10.1073/pnas.0810762106)
78. Croft DP, Edenbrow M, Darden SK, Ramnarine IW, Oosterhout C, Cable J. 2011 Effect of gyrodactylid ectoparasites on host behaviour and social network structure in guppies *Poecilia reticulata*. *Behav. Ecol. Sociobiol*. **65**, 1090–1093. (doi:10.1007/s00265-011-1230-2)
79. Heinze J, Walter B. 2010 Moribund ants leave their nests to die in social isolation. *Curr. Biol*. **20**, 249–252. (doi:10.1016/j.cub.2009.12.031)
80. Gorochowski TE, Bernardo MD, Grierson CS. 2012 Evolving dynamical networks: a formalism for describing complex systems. *Complexity* **17**, 18–25. (doi:10.1002/cplx.20386)
81. DeLellis P, Bernardo MD, Gorochowski TE, Russo G. 2010 Synchronization and control of complex networks via contraction, adaptation and evolution. *Circ. Syst. Mag. IEEE* **10**, 64–82. (doi:10.1109/MCAS.2010.937884)
82. Gorochowski TE, di Bernardo M, Grierson CS. 2010 Evolving enhanced topologies for the synchronization of dynamical complex networks. *Phys. Rev. E* **81**, 056212. (doi:10.1103/PhysRevE.81.056212)